Carbohydrate Polymers 84 (2011) 794–802

Contents lists available at ScienceDirect

Carbohydrate Polymers

journal homepage: www.elsevier.com/locate/carbpol

Preparation and characterization of radical and pH-responsive chitosan–gallic acid conjugate drug carriers

Shu-Huei Yu[a], Fwu-Long Mi[b,e,*], Jen-Chieh Pang[b], Shun-Chou Jiang[a], Tzu- Hung Kuo[b], Shao-Jung Wu[c], Shing-Shin Shyu[d]

[a] Graduate Institute of Materials Science and Technology & Department of Polymer Materials, Vanung University, Chung-Li, Taiwan, ROC
[b] Department of Biotechnology, Vanung University, Chung-Li, Taiwan, ROC
[c] Department of Chemical Engineering, MingChi University of Technology, Taipei, Taiwan, ROC
[d] Department of Cosmetic Science, Vanung University, Chung-Li 32061, Taiwan, ROC
[e] Nano Materials R&D Center, Vanung University, Chung-Li 32061, Taiwan, ROC

ARTICLE INFO

Article history:
Received 7 October 2009
Received in revised form 7 February 2010
Accepted 14 April 2010
Available online 22 April 2010

Keywords:
Chitosan
Gallic acid
Radical scavenging
PH-responsive

ABSTRACT

A novel chitosan-based nanoparticle carrier was prepared in this study. The chitosan derivative, N,O-carboxymethylchitosan (NOCC) was reacted with gallic acid (GA) using a non-toxic water-soluble carbodiimide to obtain the NOCC–GA conjugate, and the chemical structure of the conjugate was characterized with FT-IR and NMR spectra. The antioxidant activity of the NOCC–GA conjugate was examined by $DPPH^{\bullet}$ and $ABTS^{+}$ radical scavenging activity. The radical/pH-responsive properties of the NOCC–GA conjugate and its iron(II) complex were examined by fluorescence spectral and light transmittance studies. The mean particle sizes of the NOCC–GA conjugate and its iron(II) complex nanoparticles were determined by a light scattering method. The NOCC–GA conjugate and its iron(II) complex nanoparticles might provide a novel way to deliver antioxidative protein or natural products in future.

1. Introduction

Oxidative stress is the result of unregulated production of reactive oxygen species (ROS) (Finkel & Holbrook, 2000). ROS occur as a cellular mismanagement of oxidation–reduction chemistry can trigger subsequent oxidative damage to tissue and organs (Bloknina, Virolainen, & Fagerstedt, 2003). ROS are typically radicals or reactive intermediates considered to be major contributors to the cause of many diseases and ailments including aging, cardiovascular disease, ischemic injuries, and cancer (Kehrer & Smith, 1994). Antioxidants are synthetic or natural compounds that inhibit or slow the rate of oxidative damage resulting from ROS in a system. Naturally occurring antioxidants assisting in preventing oxidative damage by scavenging free radicals plays important roles as cellular antioxidants (Hemeda & Klein, 2006).

Plants, shells or microorganisms are now considered as efficient producers of antioxidative novel compounds (Chen, Zhang, Qu, & Xie, 2008; Qiao et al., 2009; Tseng, Yang, & Mau, 2008; Yuan, Zhang, Fan, & Yang, 2008). Recently, the antioxidative polysaccharides isolated from marine creatures or microorganisms have gained increasing interest (Sun et al., 2009; Zhang et al., 2009). Chitosan is a copolymer of glucosamine and N-acetylglucosamine obtained by N-deacetylation of chitin. Chitosan derivatives such as chitosan sulfate and hydroxyethyl chitosan sulfate were found to have radical scavenging activity on the DPPH, superoxide, hydroxyl radicals and carbon-centered free radicals (Huang, Mendis, & Kim, 2005; Xing et al., 2005). It was also reported that chitooligosaccharides mediated inhibition of free radical damage in cellular oxidizing systems (Mendis, Kim, Rajapakse, & Kim, 2007).

Gallic acid (GA, 3,4,5-trihydroxy benzoic acid) is a natural phenolic antioxidant extractable from natural products (Chanwitheesuk, Teerawutgulrag, Kilburn, & Rakariyatham, 2007; Lu, Nie, Belton, Tang, & Zhao, 2006). Gallic acid and its derivatives, such as tannins and catechin are widespread in plant foods exhibiting free radical scavenging effect (Lodovici et al., 2001; Leopoldini, Russo, & Toscano, 2007). Since gallic acid is regarded as a potential antioxidant, it has been used as an additive in food, drugs, and cosmetics anti-oxidation. Additionally, gallic acid was reported to possess anti-allergic, anti-inflammatory, anti-mutagenic, and anti-carcinogenic activity (Fukumoto & Mazza, 2000; Kroes, Van den Berg, Quarles van Ufford, Van Dijk, & Labadie, 1992; Shahrzad, Aoyagi, Winter, Koyama, & Bitsch, 2001).

Synthesis of antioxidant polymers by grafting of antioxidant molecules on macromolecules with biodegradability, biocompatibility, and bioactivity has received increased attention in recent

* Corresponding author at: Department of Biotechnology, Vanung University, Chung-Li 320, Taiwan, ROC. Fax: +886 3 4333063.
E-mail address: flmi530326@mail.vnu.edu.tw (F.-L. Mi).

0144-8617/$ – see front matter © 2010 Elsevier Ltd. All rights reserved.
doi:10.1016/j.carbpol.2010.04.035

times (Curcio et al., 2009; Pasanphan & Chirachanchai, 2008; Spizzirri et al., 2009; Zuo et al., 2003). Carboxymethylchitosan is a water-soluble chitosan derivative used for developing wound dressing (Chen, Wang, Chen, Ho, & Sheu, 2006), superparamagnetic nanoparticles (Liang & Zhang, 2007), hydrogels (Yin, Fei, Cui, Tang, & Yin, 2007) and fibers (Fan et al., 2006). Especially, it has proven to be a suitable polymer for controlled drug release (Chen, Tian, et al., 2004; Yin et al., 2008; Zhu et al., 2007). Low-molecular-weight carboxymethyl chitosan also showed DPPH radical and superoxide anion scavenging activity (Sun, Yao, Zhou, & Mao, 2008; Sun, Zhou, Mao, & Zhu, 2007).

The goal of this study is to develop a novel green antioxidant polymer by conjugating N,O-carboxymethylchitosan (NOCC) with gallic acid and the antioxidant polymer was used in future as a drug carrier for delivery of antioxidants. The chemical structure of NOCC–GA conjugate was characterized by ^{1}H NMR and FT-IR spectra analysis. UV absorption and free radical scavenging capability of the NOCC–GA conjugates were also investigated. The NOCC–GA conjugate was pH-sensitive and could be assembled into nanoparticles by adjusting the pH value of its solution. Self-assembly of the NOCC–GA conjugates into nanoparticles (NPs) was also triggered by Fe^{2+} and the pH/radical-responsive properties of the NPs were examined. The novel pH/radical-responsive nanoparticles will be used for deliver superoxide dismutases (SODs), an antioxidative metalloenzymes in mammalian cells, in future.

2. Materials and methods

2.1. Materials

Gallic acid was purchased from Ferak Berlin GmbH (Germany). Chitosan (MW 60 kDa) with a degree of deacetylation of approximately 85% was acquired from Koyo Chemical Co. Ltd. (Japan). Bovine serum albumin (BSA), 1,1-diphenyl-2-picrylhydrazyl (DPPH) and 2,2′-azino-bis(3-ethylbenzthiazoline-6-sulfonic acid) (ABTS) were purchased from Sigma–Aldrich Co. Ltd. (MO, USA). 1-Ethyl-3-[3-(dimethylamino)propyl]carbodiimide (EDC), N-hydroxysuccinimide (NHS), 2-(n-morpholino)ethanesulfonic acid (MES), monochloroacetic acid and all other reagents and solvents used were of reagent grade.

2.2. Synthesis of N,O-carboxymethylchitosan (NOCC)

NOCC was synthesized as per a procedure described in the literature with slight modifications (Chen, Wu, et al., 2004). Chitosan powder (10 g) was suspended in 100 ml of isopropyl alcohol and the resulting slurry was stirred in a 500-ml flask at room temperature. A 25 ml of 10 N aqueous NaOH solution, divided into five equal portions, was then added to the stirred slurry over a period of 25 min. The alkaline slurry was stirred for additional 30 min. Subsequently, monochloroacetic acid (60 g) was added, in five equal portions, at 1 min intervals. Heat was then applied to bring the reaction mixture to a temperature of 60 °C and stirring at this temperature was continued for 3 h. Afterward the reaction mixture was filtered and the filtered solid product (NOCC) was thoroughly rinsed with methanol. The resultant NOCC was dried in an oven at 60 °C.

2.3. Conjugation of NOCC with gallic acid

NOCC was synthesized from chitosan as per a procedure described in the literature with some modifications (Pasanphan & Chirachanchai, 2008). NOCC (2.18 g) was dissolved in 100 ml deionized water (DI water) and stirred overnight to obtain a NOCC solution. Gallic acid (0.01 mole) was dissolved in water/ethanol (20 ml) and 1-ethyl-3-[3-(dimethylamino)propyl]carbodiimide (EDC) in MES buffer (pH 5.5) was reacted with GA to obtain intermediate compound 1. N-Hydroxysuccinimide (NHS) was further added and the reaction was continued in an ice bath for 1 h in water to obtain intermediate compound 2. The solution of intermediate compound 2 was gradually added into the NOCC solution and stirred in an ice bath for 30 min. The reaction was carried out heterogeneously at room temperature for 24 h. The solution obtained was centrifuged, washed thoroughly with ethanol several times and dialysed against distilled water to obtain NOCC conjugated with gallic acid (NOCC–GA conjugate).

2.4. Characterization of NOCC and NOCC–GA conjugates

Fourier transformed infrared spectroscopy (FT-IR) and proton nuclear magnetic resonance spectroscopy (^{1}H NMR) was respectively used to confirm the synthesis of NOCC and NOCC–GA conjugates. The obtained NOCC or NOCC–GA conjugates used for the FT-IR analysis first was dried and ground into a powder form. The sample powder then was mixed with KBr (1:100) and pressed into a disk. Analysis was performed on an FT-IR spectrometer (Perkin Elmer Spectrum RX1 FT-IR System, Buckinghamshire, England). The sample was scanned from 400 cm^{-1} to 4000 cm^{-1}. ^{1}H NMR studies were carried out with deuterium oxide (Aldrich Chemical, Milwaukee, WI, USA). Analyses of the proton spectra were conducted on an NMR spectrometer (Varian Unityionva 500 NMR Spectrometer, MO, USA).

2.5. UV–vis measurements

NOCC–GA conjugates prepared as the aforementioned procedure were dissolved in deionized water (DI water), phosphate buffered saline (PBS) and 0.01 N aqueous NaOH were examined by scanning the sample solutions from 220 nm to 500 nm using a UV–vis spectrophotometer (Hitach 250 UV–vis, Japan) to investigate their UV absorption properties. The UV absorption properties of various concentrations of NOCC–GA conjugates (30–500 ppm in PBS) were also examined.

2.6. Antioxidant activity assay

2.6.1. Radical DPPH scavenging activity

The free radical scavenging activity was measured using 1,1-diphenyl-2-picrylhydrazyl (DPPH). Then 0.25 ml of each sample medium and 2.5 ml of reacting solution (0.35 mM DPPH in 50% ethanol) were mixed. The mixtures were left for 30 min at room temperature in the dark. Absorbencies were measured with a UV–vis spectrophotometer (Hitachi, Tokyo, Japan) at 517 nm. DPPH activity was calculated as an inhibition percentage based on the following equation:

$$\text{free radical scavenging activity}\,(\%) = \left(1 - \frac{\text{Abs}_{\text{sample}}}{\text{Abs}_{\text{control}}}\right) \times 100$$

2.6.2. Determination of antioxidant activities by $ABTS^+$

Preparation of the $ABTS^+$ radical was as described previously (Schlesier, Harwat, Bohm, & Bitsch, 2002). Then 0.25 ml of each sample medium was added to $ABTS^+$ solution (2 ml) with a blank as control sample. After mixing, the absorbance at 734 nm was measured immediately, and then every minute for 6 min. Duplicate determinations were made for triplicate samples. The percentage free radical scavenging activity was calculated from the absorbance values as abovementioned equation.

2.7. Nanoparticle self-assembly triggered by Fe^{2+}

NOCC–GA/Fe^{2+} complex nanoparticles were prepared by a Fe^{2+}-triggered self-assembly method. In brief, an aqueous $FeCl_2$ (1.5 mM) was added by flush mixing with a pipette tip into NOCC–GA conjugate solution (1.0 mg/ml, 3 ml) under magnetic stirring at room temperature. The self-assembled NOCC–GA/Fe^{2+} complex nanoparticles were collected by centrifugation at 12 000 rpm for 10 min. The mean particle sizes of nanoparticles were measured using a Zetasizer (3000HS, Malvern Instruments Ltd., Worcestershire, UK). The sample for transmission electron microscope (TEM) study was prepared by placing a drop of the nanoparticle suspension onto a 400 mesh copper grid coated with carbon. About 2 min after deposition, the grid was tapped with a filter paper to remove surface water and the morphology of nanoparticles was examined by TEM (Hitachi, H-7650, Japan).

2.8. pH/radical-responsive properties

The turbidity of the NOCC–GA conjugate or NOCC–GA/Fe^{2+} complex solutions titrated with aqueous HCl or NaOH solutions to distinct pH value, was respectively measured at $\lambda = 500$ nm with a UV–vis spectrophotometer (Uvikon923, Kontron Instruments, Italy), to examine their pH-responsive properties. The device indicated the value of transmitted light (transmittance, *T*%), system's turbidity expressed in arbitrary units as *T*%. Deionized water was used to establish the baseline. *T*% was expressed as the average of at least three measurements to investigate the stability of the nanoparticles formed in the solutions. To examine the radical-responsive property, the NOCC–GA/Fe^{2+} complex solution (3 ml) was successively added with 30 μl, 6 mM H_2O_2, and the turbidity of the complex solution was evaluated.

2.9. Fluorescence measurements

Fluorescence spectra were recorded at room temperature on a fluorescence spectrophotometer (Hitach, F-2500, Japan) to study the NOCC–GA/Fe^{2+} complex or dissociation. The NOCC–GA conjugate solutions were prepared in dilution form and the excitation wavelength was 320 nm. An aqueous $FeCl_2$ (1.5 mM, 30 μl) were added successively dropwise to 240 μl to the NOCC–GA conjugate solutions (1.0 mg/ml, 3 ml) and the fluorescence spectra were investigated. After totally quenching the fluorescence, the NOCC–GA/Fe^{2+} complex solution was added by H_2O_2 (6 mM, 30 μl) to 240 μl to examine the fluorescence recovery.

2.10. Protein loading in nanoparticles

An amount of BSA was blended with aqueous NOCC–GA conjugate solutions with thoroughly stirring to obtain the BSA/NOCC–GA mixture (0.1 mg/ml BSA and 1.0 mg/ml NOCC–GA conjugate, 3 ml). The mixed solution was added with 1000 μl of $FeCl_2$ (1.5 mM) under magnetic stirring at room temperature and the obtained BSA-containing nanoparticles were collected as described before. The supernatants were analyzed by the Bradford method for BSA at 595 nm to determine the drug loading efficiency (Bradford, 1976).

3. Results and discussion

3.1. Characterization of NOCC and NOCC–GA conjugate

Fig. 1(A) shows the FT-IR spectra of chitosan, NOCC, GA and NOCC–GA conjugates. NOCC is a water-soluble chitosan derivative having carboxymethyl substituents on some of both the amino and primary hydroxyl sites of the glucosamine units of the chitosan structure. NOCC showed a characteristic peak (1601 cm^{-1}) for associated carboxylic acid salt (–COO^- antisym stretch), suggesting the substitution of carboxymethyl groups on NOCC. The peaks observed at 1070 cm^{-1} and 1029 cm^{-1} were the secondary hydroxyl group (characteristic peak of –CH–OH in cyclic alcohols, C–O stretch) and the primary hydroxyl group (characteristic peak of –CH_2–OH in primary alcohols, C–O stretch), respectively. The decrease of peak area ratios (1029/1070 cm^{-1}) of chitosan subsequent to carboxymethylation of chitosan (NOCC) is the evidence

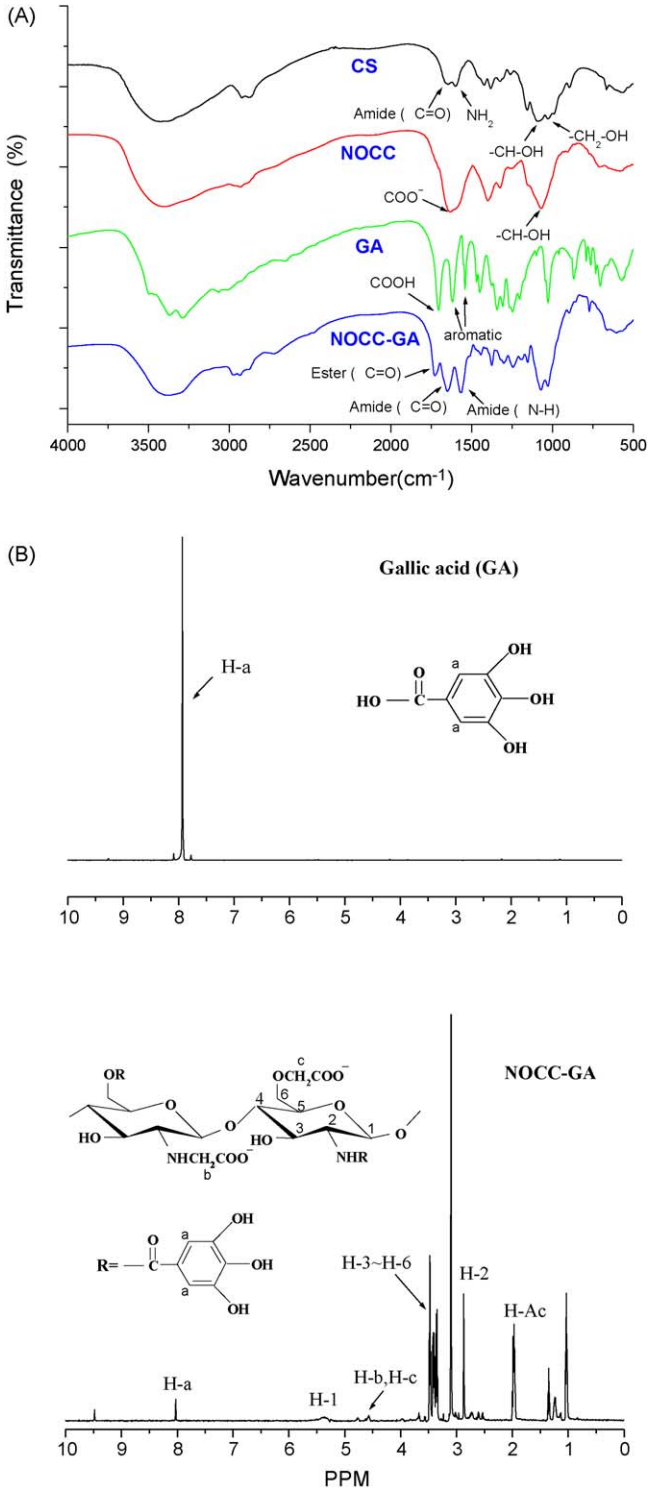

Fig. 1. (A) FT-IR spectra and (B) NMR spectra of NOCC, GA and NOCC–GA conjugate.

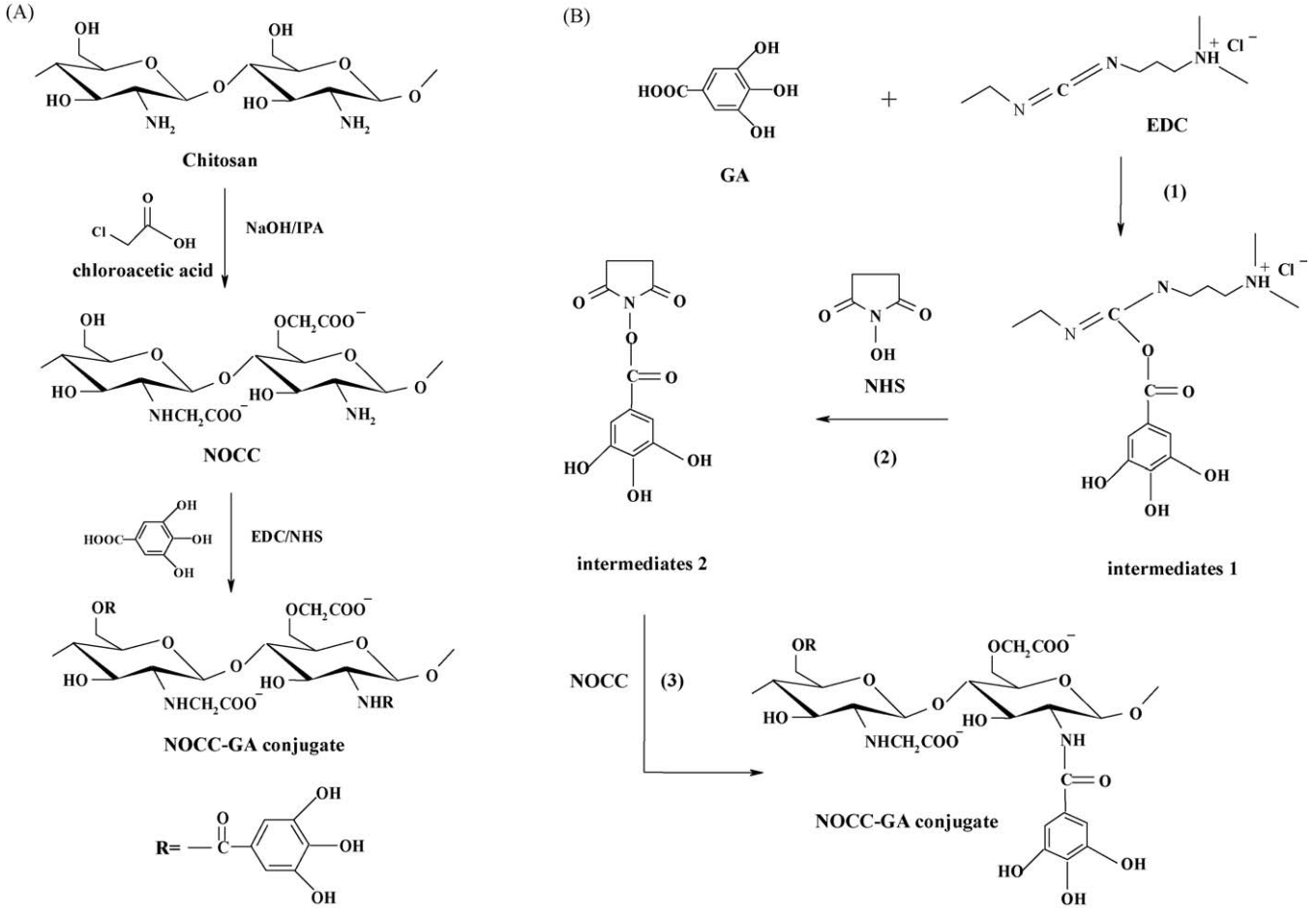

Fig. 2. The schematic reaction mechanism for the synthesis of NOCC–GA conjugates using EDC/NHS. (A) The total synthesis procedure of NOCC–GA conjugates. (B) Substitution of GA onto NOCC: carboxyl groups on GA react with EDC to produce the intermediate, O-acylisourea (intermediate 1). The O-acylisourea will react with NHS to produce the intermediate active ester (intermediate 2, the product of condensation of the carboxylic group and N-hydroxysuccinimide) that further reacts with the amino groups on NOCC to yield final amide bonding product.

that a carboxymethyl group was substituted to $-CH_2-OH$ at the C-6 position of the chitosan derivative (NOCC).

The schematic mechanism for the synthesis of NOCC–GA conjugates was shown in Fig. 2(A). EDC initiated the reactive carboxyl groups on GA. The nucleophilic reaction possibly occurs at C-2 (primary amines) and C-6 (primary alcohols). *N*-Hydroxysuccinimide (NHS) is often used to assist the carbodiimide coupling in the presence of EDC. The reaction includes formation of the intermediate active ester (the product of condensation of the carboxylic group and *N*-hydroxysuccinimide) that further reacts with the amine function to yield finaly the amide bond (Fig. 2(B)). NOCC–GA conjugate showed the characteristic peaks at 1730 cm^{-1} (ester) or 1640 cm^{-1} (amide), suggesting the conjugation of GA on NOCC is at either C-2 (via the formation of amide linkage), or C-6 (via the formation of ester linkage).

The proton NMR spectra of GA and synthesized NOCC–GA conjugate are presented in Fig. 1(B). As shown in the spectrum of the NOCC–GA conjugate, the chemical shifts at 4.2 ppm and 4.4 ppm were the protons at C-2 and C-6 of the chitosan derivative (NOCC), respectively. The low intensity of both peaks indicated that the protons on the amino and primary hydroxyl sites of the modified chitosan structure were almost substituted by the carboxymethyl groups and GA. The peaks of protons on phenol hydroxyl groups and carboxyl group of GA are very weak. A two-proton singlet at 7.9 ppm relates to the protons on benzene ring was significant which could be assigned to the substituted GA in the NMR spectra of the NOCC–GA conjugate (shift to 8.0 ppm after conjugation). The GA substitution degree determined from the NMR spectra was 10.3%.

3.2. Characterization of UV absorption and antioxidant activity

Fig. 3 shows the UV–vis spectra of NOCC–GA conjugates. It has been reported that the absorption spectrum of GA aqueous solution exhibits two peaks at 225 nm and 260 nm. Indeed, GA in DI water showed two peaks at 223 nm and 259 nm but the peak at 259 nm shift to 284 nm in 0.01 N NaOH (aq) because GA will dissociated to form phenoxide ions ($Ar-O^-$) caused by ionization of the GA molecule. (Fig. 3(A)). It was found that NOCC–GA conjugates could be dissolved in 0.01 N NaOH (aq) and displayed the same red shift of the peak from 259 nm to 299 nm (Fig. 3(A)). Absorption spectra of NOCC–GA conjugates in PBS showed that the characteristic peak at 261 nm and 293 nm increased with the increase of NOCC–GA concentrations suggesting the superior UV absorption properties (Fig. 3(B)). This is due to the fact that the phenol hydroxyl groups (the p*K*a of phenol is 9.95) will dissociated in alkaline solution or PBS buffer that may exhibit different GA forms (phenoxide ions or quinones) caused by ionization (from Ar–OH to $Ar-O^-$) or oxidation of the GA molecule. The NOCC–GA conjugate solution became turbid and NPs formed under the condition of adding Fe^{2+} into the NOCC–GA solution therefore decrease the absorption (Fig. 3(A)).

The antioxidant activities of prepared NOCC–GA conjugates were measured in the DPPH• or $ABTS^+$ radical system and were expressed as RS(%) (Fig. 4(A) and (B)). RS(%) is the DPPH• or $ABTS^+$

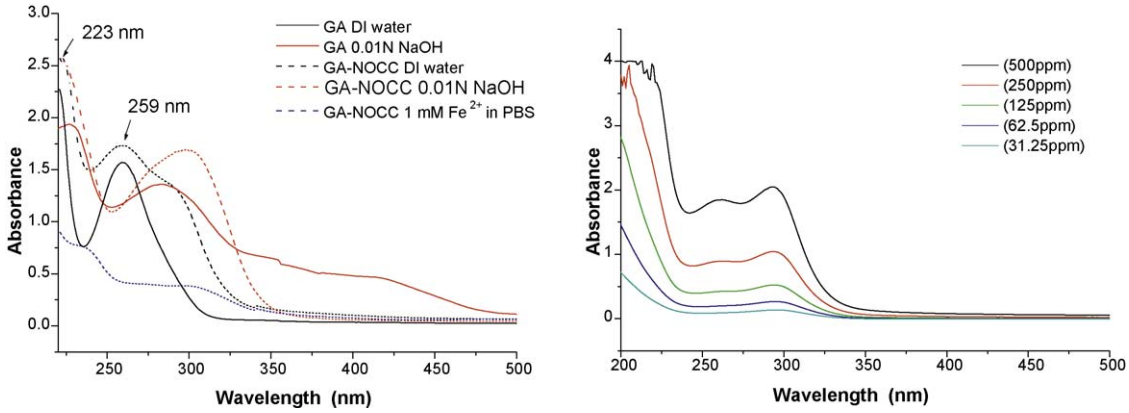

Fig. 3. Effects of the solution property and concentration on the UV absorption properties of the NOCC–GA conjugate. (A) GA and NOCC–GA conjugates dissolved in DI water, 0.01 N NaOH and 1 mM Fe^{2+}/PBS aqueous solutions. (B) Various concentrations of NOCC–GA conjugates dissolved in PBS.

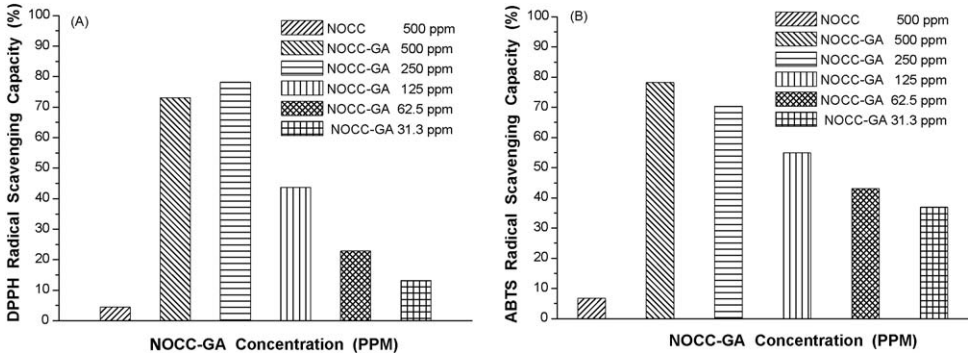

Fig. 4. (A) DPPH• free radical scavenging activity and (B) $ABTS^+$ free radical scavenging activity of NOCC–GA conjugates.

radical scavenging percentage (%) in the reaction mixtures. A higher RS(%) value is associated with a stronger DPPH• scavenging activity. NOCC demonstrated a lower RS(%) value (4.5% by using 500 μg/ml of NOCC). The NOCC–GA conjugates showed superior DPPH• scavenging activity. The RS(%) value of NOCC–GA conjugate increases as the concentration increases and is up to 73% when the concentration reached 500 μg/ml. The RS(%) value determined from the $ABTS^+$ radical system was 78% using 500 μg/ml of NOCC–GA conjugate. The EC_{50} value, which expresses the antioxidant concentration to reduce the $ABTS^+$ radicals by 50%, is 219 μg/ml. The results of DPPH• and $ABTS^+$ radical scavenging activities implies the function of NOCC–GA conjugate as an antioxidative polymer.

3.3. Fe^{2+}-triggered self-assembly of nanoparticles

Fig. 5(A) shows that the fluoresence intensity of the NOCC–GA solution decreased after the addition of H_2O_2. Fig. 5(B) shows the effect of iron coordination on the fluorescence property of the NOCC–GA conjugate. The phenol hydroxyl groups (Ar–OH) of GA are known to be suitable ligands for iron(II) and iron(III) ions (Khokhar & Apenten, 2003). In this work, the formation of NOCC–GA/Fe^{2+} complex was believed to occur through the coordination at the phenol hydroxyl groups and also the carboxymethyl groups of NOCC. The fluorescence bands of the phenol hydroxyl groups π-system are charge transfer in character; therefore, fluorescence emission should be affected if Fe^{2+} bind to the phenol hydroxyl groups. The emission maximum of the NOCC–GA conjugate was at 368 nm while the excitation wavelength was 316 nm. Once Fe^{2+} coordination has occurred, fluorescence quenching can be caused by the variation of electron density on the phenol hydroxyl groups. This result is the evidence for the formation of NOCC–GA/Fe^{2+} complex.

In contrast, a deep fluorescence quenching followed with slow fluorescence recovery (the emission was red-shift to 455 nm) could be observed from the NOCC–GA/Fe^{2+} complex solution after the addition of hydrogen peroxide (H_2O_2) (Fig. 5(C)). The fluorescence quenching might be due to the oxidation of NOCC–GA conjugates by H_2O_2, while the followed fluorescence recovery should be due to the transformation of iron coordination type of the NOCC–GA complex (Ar–OH → .Ar=O; Fe^{2+} → $.Fe^{3+}$).

The NOCC–GA conjugate solution became turbid and NPs formed under the condition of adding Fe^{2+} into the NOCC–GA solution. NOCC NPs synthesized by simple ionic cross-linking using TPP and $CaCl_2$ showed less cytotoxicity but effective antibacterial activity (Anitha et al., 2009). As shown in Table 1, the mean particle size decreased but light scattering increased with the increase of added Fe^{2+} concentration. This result suggested that the metal ion (Fe^{2+}) coordination of the phenol hydroxyl groups on gallic acid and the carboxymethyl groups on NOCC triggered the self-assembly of NPs. The decrease of mean particle size indicates denser nanoparticles (less swellable) were obtained from the NOCC–GA/Fe^{2+} complex with increased Fe^{2+} contents because its high cross-linking density. Fig. 5(D) shows the TEM micrography of

Table 1
Mean particle size of self-assembled NOCC–GA/Fe^{2+} complex NPs via the addition of different amounts of Fe^{2+} ions (1.5 mM).

Fe^{2+} (μl)	Particle size (nm)	Static scattering	Dynamic scattering
200	2010.8	53.7	22.7
400	859.6	76.6	55.1
600	693.6	105.6	91.6
800	548.1	189.8	159.2
1000	534.1	166.6	130.4

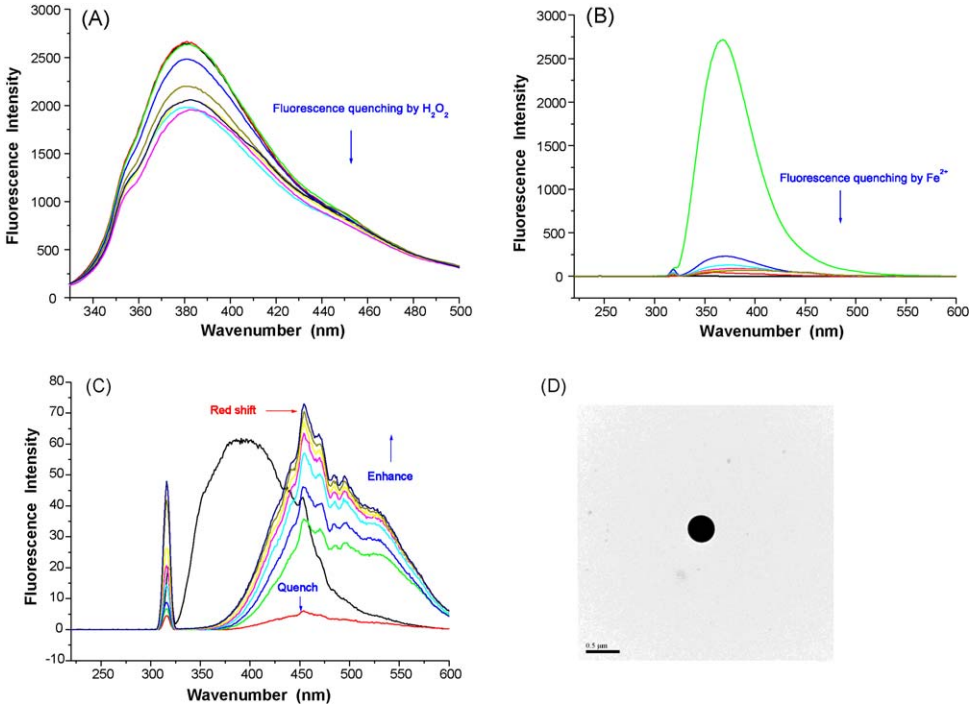

Fig. 5. Effects of coordination with Fe^{2+} and oxidation by H_2O_2 on the fluorescence properties of NOCC–GA conjugate solutions. (A) An aqueous H_2O_2 (6 mM, 30 μl) was added successively dropwise to 240 μl to the NOCC–GA conjugate solution. (B) An aqueous FeCl2 (1.5 mM, 30 μl) were added successively dropwise to 240 μl to the NOCC–GA conjugate solutions (1.0 mg/ml, 3 ml). (C) An aqueous H_2O_2 (6 mM, 30 μl) was added successively dropwise to 240 μl to the previously fluorescence quenched NOCC–GA/Fe^{2+} complex solution. (D) TEM morphology of NOCC–GA/Fe^{2+} complex nanoparticles prepared by adding 1000 μl to the NOCC–GA conjugate solutions (1.0 mg/ml, 3 ml), the scale is 0.5 μm.

the prepared NOCC–GA/Fe^{2+} complex nanoparticles. The nanoparticles are spherical and intact in morphology.

3.4. pH/radical-responsive properties of prepared nanoparticles

The NOCC–GA conjugate is a pH-responsive polymer. As shown in Fig. 6(A), the critical pH condition for solution became turbid might be in the range of pH 3.2–4.0 ($T\% < 12.0$), indicating self-assembly of the macromolecule into NPs. In the pH range, the self-assembled NOCC–GA conjugate NPs was very stable because the electrostatic interaction between the carboxyl and amino groups on NOCC macromolecular chains. When pH value decreased to 3.0, light transmittance ($T\%$) of the NOCC–GA conjugate solution increased to 58%. Most carboxylic groups of NOCC were in form of –COOH while the amino groups were protonated. Hence, there was little electrostatic interaction between the carboxyl and amino groups. At this pH condition, self-assembly of the macromolecule depends on the balance of hydrophilic amino/hydroxyl groups and the conjugated hydrophobic gallic acid. When pH value decreased to 2.0, $T\%$ of the NOCC–GA conjugate solution increased to higher than 90%. This indicated no more electrostatic interaction in the NOCC–GA conjugate and the NPs became unstable and subsequently broken apart.

Fig. 6(A) also shows the pH/radical-responsive properties of the NOCC–GA/Fe^{2+} complex solutions. Proton dissociation of phenol hydroxyl and carboxyl groups, in relation to the structure and activity of GA, is responsible for the iron(III)–GA complex stability (Ji, Zhang, & Shen, 2006). The turbidity of NOCC–GA/Fe^{2+} complex solution was high and showed no apparent change ($T\% < 22\%$) in the pH range of 2.4–7.4. $T\%$ of the solution increased to 91% as the acidity increased to pH 1.2, suggesting the dissociation of NOCC–GA/Fe^{2+} complex.

The pKa value of carboxymethyl group ranges 3.55–4.10. The transmittance increases as pH is larger than 4 for NOCC–GA conju-

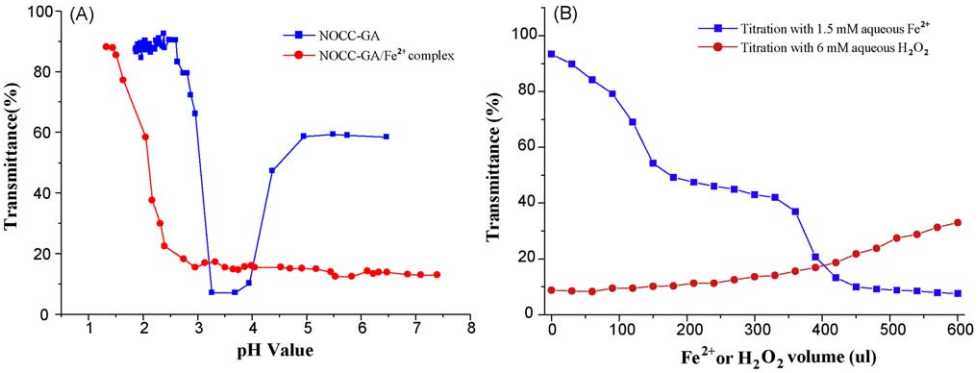

Fig. 6. (A) pH-responsive turbidity of NOCC–GA conjugate and NOCC–GA/Fe^{2+} complex solutions. (B) Turbidity of the NOCC–GA conjugate solution by added with an aqueous FeCl2 (1.5 mM, 30 μl) and the radical-responsive turbidity of the NOCC–GA//Fe^{2+} complex solution by added with an aqueous H_2O_2 (6 mM, 30 μl).

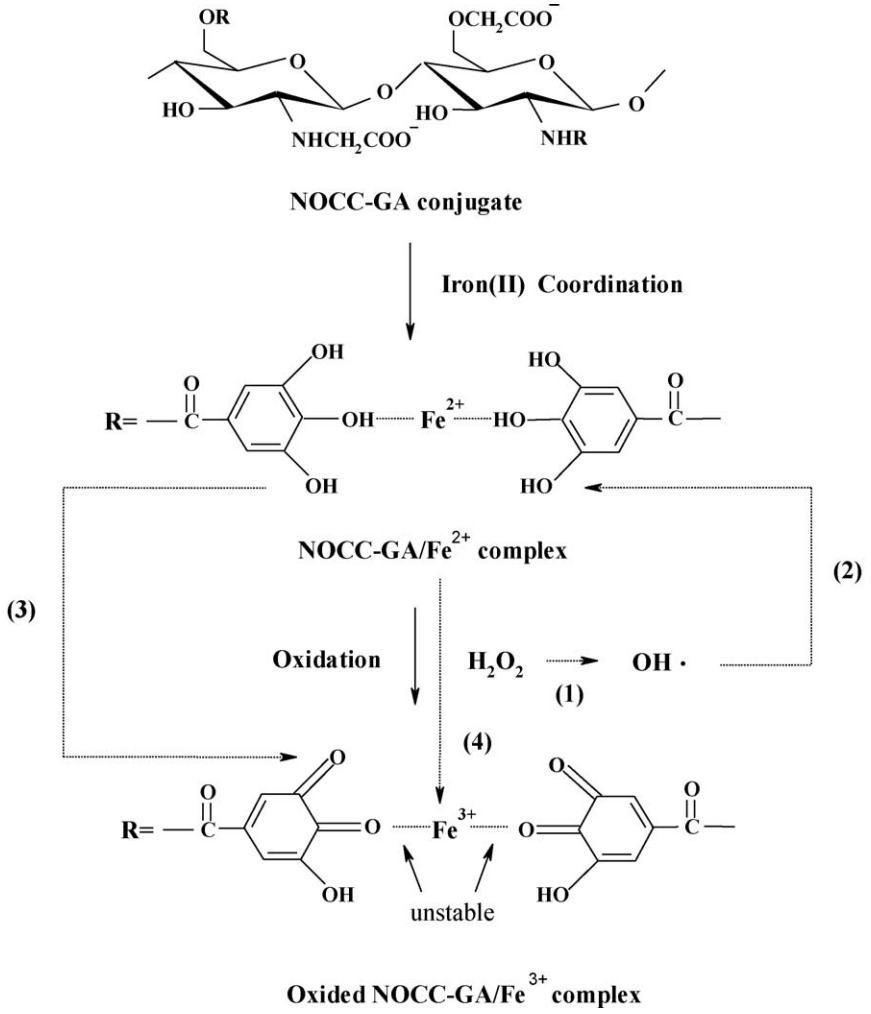

Fig. 7. The schematic reaction mechanism for the dissociation of NOCC–GA/Fe^{2+} complexes in the presence of H_2O_2. Iron(II) ions coordinated at the phenol hydroxyl of the substituted GA on NOCC. H_2O_2 will convert into the hydroxyl radical (1), resulted in the oxidation of the aromatic hydroxyl (2) to form quinines (3) accompanied with the conversion of coordinated Fe^{2+} ions to Fe^{3+} ions (4). The NOCC–GA/Fe^{2+} complexes became instable and gradually dissociated.

gate because the carboxymethyl groups (–CH_2COOH) was ionized to carboxylic ions (–CH_2COO^-). In contrast, the carboxymethyl groups of NOCC in the NOCC–GA/Fe^{+2} complexes were coordinated with Fe^{+2} to form a stable structure. Therefore, the transmittance remains low in the pH range of 2.4–7.4 because the NOCC–GA/Fe^{+2} complex nanoparticles were stable in the pH range. However, *T*% of the NOCC–GA/Fe^{2+} complex solution gradually increased when H_2O_2 was added into the solution (Fig. 6(B)). It was known that in the presence of trace amounts of iron(II), H_2O_2 will convert into the hydroxyl radical and initiate the oxidation of organic substrates. In this study, the addition of H_2O_2 to the aqueous solution of NOCC–GA/Fe^{2+} complex resulted in the oxidation of the aromatic hydroxyl (Ar–OH) to quinones (Ar=O) accompanied with the conversion of coordinated Fe^{2+} ions to Fe^{3+} ions (Fig. 7). The NPs became unstable and subsequently disintegrated due to the dissociation of the NOCC–GA/Fe^{2+} complex.

3.5. Protein loading

Superoxide dismutases (SODs) are a family of antioxidative metalloenzymes present in all mammalian cells. SODs convert superoxide anion into hydrogen peroxide, which are subsequently degraded by catalase, giving water and molecular oxygen. However, SODs are instable and rapidly inactivated, resulting in a very short plasma half-life ($t_{1/2}$ < 6 min). Therefore, an appropriate drug carrier able to effectively load the enzyme and protect the enzyme against inactivation is desired.

BSA was used as a model protein in this study to examine the possibility of using the NOCC–GA/Fe^{2+} complex nanoparticles as a protein drug carrier. The loading efficiency of BSA in nanoparticles was about 82.8 ± 6.2%. Such a high loading efficiency is possibly due to the fact that Fe^{2+} ions are able to associate with BSA/Fe^{2+}complex (Arakawa & Kimura, 1979). Additionally, polyphenols containing GA units is known to bind with proteins via non-covalent interactions (Siebert, Troukhanova, & Lynn, 1996). As shown in the TEM micrograph (Fig. 8), the NOCC–GA/Fe^{2+} complex nanoparticles were spherical in shape. However, the BSA-containing NOCC–GA/Fe^{2+} complex nanoparticles became smaller and the resulting nanoparticles aggregates were observed from the TEM micrograph. Therefore, it still needs more studies to examine the impact of the NOCC–GA conjugate for used as protein delivery carriers.

NOCC is water-soluble but CS only dissolved in acid. The substituted carboxymethyl group on the NOCC–NOCC–GA conjugate played as a proton donor-receptor providing the pH-responsive property of NOCC. Additionally, the carboxymethyl groups associated with the aromatic hydroxyl groups on GA for Fe^{2+}

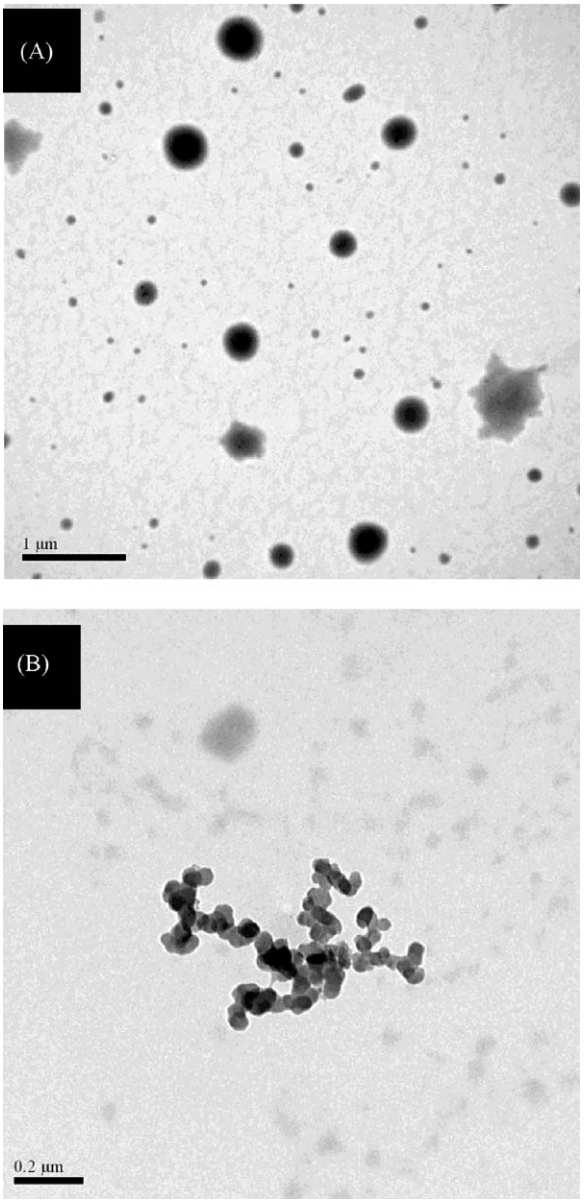

Fig. 8. TEM micrography of the NOCC–GA/Fe^{2+} complex nanoparticles. (A) Nanoparticles prepared by the same method, the scale is 1 μm. (B) BSA-containing NOCC–GA/Fe^{2+} complex. Nanoparticles prepared by adding 1000 μl of Fe^{2+} ions (1.5 mM) to the mixture of BSA and NOCC–GA conjugate solutions (0.1 mg/ml BSA and 1.0 mg/ml NOCC–GA conjugate, 3 ml), the scale is 0.2 μm.

coordination, leading to the formation of nanoparticles and the conversion of H_2O_2 into the hydroxyl radical. The substituted GA on NOCC was oxidized from phenol to quinone structure accompanied with the scavenging of hydroxyl radical.

4. Conclusion

In this study, a NOCC–GA conjugate with antioxidative capability was synthesized. We found that Fe^{2+} could trigger the self-assembly of the NOCC–GA conjugate into NOCC–GA/Fe^{2+} complex NPs. The complex NPs were radical/pH-responsive and were able to load a model protein, BSA. Such a novel nanoparticle carrier may be used to deliver antioxidative protein or natural products in future.

Acknowledgement

The financial support for this research was provided by the National Science Council (NSC 97-2221-E-238-002-MY2), Taiwan, ROC.

References

Anitha, A., Divya Rani, V. V., Krishna, R., Sreeja, V., Selvamurugan, N., Nair, S. V., et al. (2009). Synthesis, characterization, cytotoxicity and antibacterial studies of chitosan, O-carboxymethyl and N,O-carboxymethyl chitosan nanoparticles. *Carbohydrate Polymers*, *78*, 672–677.

Arakawa, S., & Kimura, T. (1979). Preparation and partial characterization of iron–sulfur, iron–selenium, and iron–tellurium complexes of bovine serum albumin. *Biochimica et Biophysica Acta (BBA)—Protein Structure*, *580*, 382–391.

Bloknina, O., Virolainen, E., & Fagerstedt, K. V. (2003). Antioxidants, oxidative damage and oxygen deprivation stress: A review. *Annals of Botany*, *91*, 179–194.

Bradford, M. M. (1976). A rapid and sensitive method for the quantitation of microgram quantities of protein utilizing the principle of protein–dye binding. *Analytical Biochemistry*, *72*, 248–254.

Chanwitheesuk, A., Teerawutgulrag, A., Kilburn, J. D., & Rakariyatham, N. (2007). Antimicrobial gallic acid from Caesalpinia mimosoides Lamk. *Food Chemistry*, *100*, 1044–1048.

Chen, L., Tian, Z., & Du, Y. (2004). Synthesis and pH sensitivity of carboxymethyl chitosan-based polyampholyte hydrogels for protein carrier matrices. *Biomaterials*, *25*, 3725–3732.

Chen, S. C., Wu, Y. C., Mi, F. L., Lin, Y. H., Yu, L. C., & Sung, H. W. (2004). A novel pH-sensitive hydrogel composed of N, O-carboxymethyl chitosan and alginate cross-linked by genipin for protein drug delivery. *Journal of Controlled Release*, *96*, 285–300.

Chen, R. N., Wang, G. M., Chen, C. H., Ho, H. O., & Sheu, M. T. (2006). Development of N,O-carboxymethylchitosan/collagen matrixes as a wound dressing. *Biomacromolecules*, *7*, 1058–1064.

Chen, H., Zhang, M., Qu, Z., & Xie, B. (2008). Antioxidant activities of different fractions of polysaccharide conjugates from green tea (Camellia sinensis). *Food Chemistry*, *106*, 559–563.

Curcio, M., Puoci, F., Iemma, F., Parisi, O. I., Cirillo, G., Spizzirri, U. G., et al. (2009). Covalent insertion of antioxidant molecules on chitosan by free radical grafting procedure. *Journal of Agricultural and Food Chemistry*, *57*, 5933–5938.

Fan, L., Du, Y., Zhang, B., Yang, J., Zhou, J., & Kennedy, J. F. (2006). Preparation and properties of alginate/carboxymethyl chitosan blend fibers. *Carbohydrate Polymers*, *65*, 447–452.

Finkel, T., & Holbrook, N. J. (2000). Oxidants, oxidative stress and the biology of aging. *Nature*, *408*, 239–247.

Fukumoto, L. R., & Mazza, G. J. (2000). Assessing antioxidant and prooxidant activities of phenolic compounds. *Journal of Agricultural and Food Chemistry*, *48*, 3597–3604.

Hemeda, H. M., & Klein, B. P. (2006). Effects of naturally occurring antioxidants on peroxidase activity of vegetable extracts. *Journal of Food Science*, *55*, 184–185.

Huang, R., Mendis, E., & Kim, S. K. (2005). Factors affecting the free radical scavenging behavior of chitosan sulfate. *International Journal of Biological Macromolecules*, *36*, 120–127.

Ji, H. F., Zhang, H. Y., & Shen, L. (2006). Proton dissociation is important to understanding structure–activity relationships of gallic acid antioxidants. *Bioorganic and Medical Chemistry Letters*, *16*, 4095–4098.

Kehrer, J. P., & Smith, C. V. (1994). Free radicals in biology: Sources, reactivity, and role in the etiology of human diseases. In *Natural antioxidants in human health and disease*. New York: Academic Press., pp. 25–62.

Khokhar, S., & Apenten, R. K. O. (2003). Iron binding characteristics of phenolic compounds: Some tentative structure–activity relations. *Food Chemistry*, *81*, 133–140.

Kroes, B. H., Van den Berg, A. J. J., Quarles van Ufford, H. C., Van Dijk, H., & Labadie, R. P. (1992). Anti-inflammatory of gallic acid. *Planta Medica*, *58*, 499–504.

Leopoldini, M., Russo, N., & Toscano, M. A. (2007). A comparative study of the antioxidant power of flavonoid catechin and its planar analogue. *Journal of Agricultural and Food Chemistry*, *55*, 7944–7949.

Liang, Y. Y., & Zhang, L. M. (2007). Bioconjugation of papain on superparamagnetic nanoparticles decorated with carboxymethylated chitosan. *Biomacromolecules*, *8*, 1480–1486.

Lodovici, M., Guglielmi, F., Casalini, C., Meoni, M., Cheynier, V., & Dolara, P. (2001). Antioxidant and radical scavenging properties in vitro of polyphenolic extracts from red wine. *European Journal of Nutrition*, *40*, 74–77.

Lu, Z., Nie, G., Belton, P. S., Tang, H., & Zhao, B. (2006). Structure–activity relationship analysis of antioxidant ability and neuroprotective effect of gallic acid derivatives. *Neurochemistry International*, *48*, 263–274.

Mendis, E., Kim, M. M., Rajapakse, N., & Kim, S. K. (2007). An in vitro cellular analysis of the radical scavenging efficacy of chitooligosaccharides. *Life Sciences*, *80*, 2118–2212.

Pasanphan, W., & Chirachanchai, S. (2008). Conjugation of gallic acid onto chitosan: An approach for green and water-based antioxidant. *Carbohydrate Polymers*, *72*, 169–177.

Qiao, D., Ke, C., Hu, B., Gan, D., Luo, J., Ye, H., et al. (2009). Antioxidant activities of polysaccharides from Hyriopsis cumingi. *Carbohydrate Polymers*, *78*, 199–204.

Schlesier, K., Harwat, M., Bohm, V., & Bitsch, R. (2002). Assessment of antioxidant activity by using different in vitro methods. *Free Radical Research*, *36*, 177–187.
Shahrzad, S., Aoyagi, K., Winter, A., Koyama, A., & Bitsch, I. (2001). Pharmacokinetics of gallic acid and its relative bioavailability from tea in healthy humans. *Journal of Nutrition*, *131*, 1207–1210.
Siebert, K. J., Troukhanova, N. V., & Lynn, P. Y. (1996). Nature of polyphenol–protein interactions. *Journal of Agriculture and Food Chemistry*, *44*, 80–85.
Spizzirri, U. G., Iemma, F., Puoci, F., Cirillo, G., Curcio, M., Parisi, O. I., et al. (2009). Synthesis of antioxidant polymers by grafting of gallic acid and catechin on gelatin. *Biomacromolecules*, *10*, 1923–1930.
Sun, T., Zhou, D., Mao, F., & Zhu, Y. (2007). Preparation of low-molecular-weight carboxymethyl chitosan and their superoxide anion scavenging activity. *European Polymer Journal*, *43*, 652–656.
Sun, T., Yao, Q., Zhou, D., & Mao, F. (2008). Antioxidant activity of *N*-carboxymethyl chitosan oligosaccharides. *Bioorganic & Medicinal Chemistry Letters*, *18*, 5774–5776.
Sun, H. H., Mao, W. J., Chen, Y., Guo, S. D., Li, H. Y., Qi, X. H., et al. (2009). Isolation, chemical characteristics and antioxidant properties of the polysaccharides from marine fungus Penicillium sp. F23-2. *Carbohydrate Polymers*, *78*, 117–124.
Tseng, Y. H., Yang, J. H., & Mau, J. L. (2008). Antioxidant properties of polysaccharides from Ganoderma tsugae. *Food Chemistry*, *107*, 732–738.
Xing, R. E., Liu, S., Guo, Z. Y., Yu, H. H., Wang, P. B., Li, C. P., et al. (2005). Relevance of molecular weight of chitosan and its derivatives and their antioxidant activities in vitro. *Bioorganic & Medicinal Chemistry*, *13*, 1573–1577.
Yin, L., Fei, L., Cui, F., Tang, C., & Yin, C. (2007). Superporous hydrogels containing poly(acrylic acid-co-acrylamide)/O-carboxymethyl chitosan interpenetrating polymer networks. *Biomaterials*, *28*, 1258–1266.
Yin, L., Ding, J. Y., Fei, L., Heb, M., Cui, F., Tang, C., et al. (2008). Beneficial properties for insulin absorption using superporous hydrogel containing interpenetrating polymer network as oral delivery vehicles. *International Journal of Pharmaceutics*, *350*, 220–229.
Yuan, J. F., Zhang, Z. Q., Fan, Z. C., & Yang, J. X. (2008). Antioxidant effects and cytotoxicity of three purified polysaccharides from Ligusticum chuanxiong Hort. *Carbohydrate Polymers*, *74*, 822–827.
Zhang, Z., Zhang, Q., Wang, J., Shi, X., Song, H., & Zhang, J. (2009). In vitro antioxidant activities of acetylated, phosphorylated and benzoylated derivatives of porphyran extracted from Porphyra haitanensis. *Carbohydrate Polymers*, *78*, 449–453.
Zhu, A., Jin, W., Yuan, L., Yang, G., Yu, H., & Wu, H. (2007). *O*-Carboxymethylchitosan-based novel gatifloxacin delivery system. *Carbohydrate Polymers*, *68*, 693–700.
Zuo, X. L., Chen, J. M., Zhou, X., Li, X. Z., Mei, G. Y., Chung, J. E., et al. (2003). Enzymatic synthesis and antioxidant property of gelatin–catechin conjugates. *Biotechnolgy Letter*, *25*, 1993–1997.